HHS Public Access

Author manuscript

J Nat Prod. Author manuscript; available in PMC 2018 March 24.

Published in final edited form as:

J Nat Prod. 2017 March 24; 80(3): 659–669. doi:10.1021/acs.jnatprod.6b01150.

(+)-Strebloside-induced Cytotoxicity in Ovarian Cancer Cells is Mediated through Cardiac Glycoside Signaling Networks

Wei-Lun Chen[†], **Yulin Ren**[‡], **Jinhong Ren**[†], **Christian Erxleben**[§], **Michael E. Johnson**[†], **Saverio Gentile**[§], **A. Douglas Kinghorn**[‡], **Steven M. Swanson**[†,⊥], and **Joanna E. Burdette**[*,†]

[†]Department of Medicinal Chemistry and Pharmacognosy, College of Pharmacy, University of Illinois at Chicago, Chicago, IL 60612, United States

[‡]Division of Medicinal Chemistry and Pharmacognosy, College of Pharmacy, The Ohio State University, Columbus, OH 43210, United States

[§]Department of Molecular Pharmacology & Therapeutics, Loyola University, Chicago, IL 60153, United States

[⊥]School of Pharmacy, University of Wisconsin-Madison, Madison, WI 53705, United States

Abstract

(+)-Strebloside, a cardiac glycoside isolated from the stem bark of *Streblus asper* collected in Vietnam, has shown some potential for further investigation as an antineoplastic agent. A mechanistic study using an in vitro assay and molecular docking analysis, indicated that (+)-strebloside binds and inhibits Na^+/K^+-ATPase in a similar manner to digitoxin. Inhibition of growth of different high-grade serous ovarian cancer cells including OVCAR3, OVSAHO, Kuramochi, OVCAR4, OVCAR5, and OVCAR8 resulted from treatment with (+)-strebloside. Furthermore, this compound blocked cell cycle progression at the G2-phase and induced PARP cleavage indicating apoptosis activation in OVCAR3 cells. (+)-Strebloside potently inhibited mutant p53 expression through the induction of ERK pathways and inhibited NF-κB activity in human ovarian cancer cells. However, in spite of its antitumor potential, the overall biological activity of (+)-strebloside must be regarded as being typical of better-known cardiac glycosides such as digoxin and ouabain. Further chemical alteration of cardiac glycosides might help to reduce negative side effects while increasing cancer cell cytotoxicity.

Graphical abstract

[*]**Corresponding Author** joannab@uic.edu; Tel: 312-996-6153.

Supporting information

The Supporting Information is available free of charge on the ACS Publications website

ORCID

Joanna E. Burdette: 0000-0002-7271-6847.

Notes

The authors declare no competing financial interest.

DEDICATION

Dedicated to Professor Phil Crews, of the University of California, Santa Cruz, for his pioneering work on bioactive natural products.

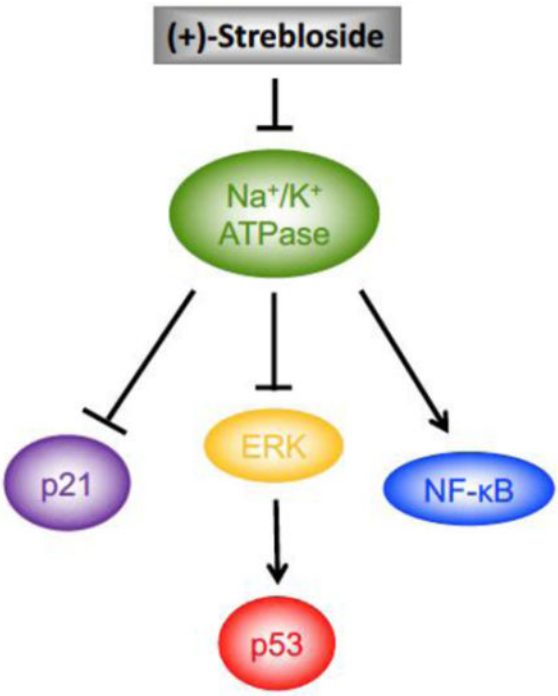

Drug repurposing is a strategy that offers promising opportunities for increasing the number of small molecules that can be used to treat disease. Extensive searches for potent anticancer drug leads have revealed that some drugs can be repurposed for cancer. Cardiac glycosides, such as digoxin, are prescribed to treat cardiovascular disease, but they also display anticancer activity. Thus, lower mortality rates have been reported in women with breast cancer treated with cardiac glycosides as compared to those not consuming these compounds.[1] Epidemiologic studies have demonstrated a reduced incidence of leukemia, lymphoma, renal, prostate, and lung cancer with regular cardiac glycoside intake.[2, 3] Other reports have indicated that cardiac glycosides may exhibit synergistic anticancer-related effects when used in combination with chemotherapeutic agents. For example, a combination of the cardiac glycoside oleandrin and cisplatin resulted in greater cytotoxicity in prostate, breast, lung, pancreatic, colorectal, and melanoma cell lines than either agent alone.[4] A synergistic cytotoxic effect was observed in a human colon cancer cell line when digoxin was combined with oxaliplatin.[5] Several cardiac glycosides have been studied in clinical trials as potential anticancer treatments.[6] However, in contrast to some of the positive studies, in the Surveillance, Epidemiology and End-Results (SEER)-Medicare database analysis, digoxin use during chemotherapy was not associated with improved overall survival in patients with epithelial ovarian cancer treated with surgery and platinum chemotherapy.[7] A recent study revealed that bufalin induces cell cycle arrest and apoptosis in endometrial and ovarian cancer.[8] However, little has been studied on cardiac glycosides in high-grade serous ovarian cancer (HGSC), which is the most common and lethal form of ovarian cancer.

Cardiac glycosides are a class of chemical compounds used clinically for arrhythmia and heart failure that specially inhibit Na^+/K^+-ATPase. Apart from its function on the ion pump,

Na^+/K^+-ATPase interacts with different signaling proteins and many of these have been studied for their role in reducing cancer cell viability. Inhibition of Na^+/K^+-ATPase induced Ca^{2+} accumulation and increased reactive oxygen species (ROS), followed by growth arrest and cell death. Na^+/K^+-ATPase inhibition also activated signal transduction pathways including Src, EGFR, and MAPK, and reduced p53 synthesis.[9-12] A study on hepatocellular carcinoma using quantitative proteomics and bioinformatics showed several proteins involved in the mitotic cell cycle (e.g., cyclin D1 and CDK) and in chromosome segregation (e.g., AURKA and SMC2) were primarily decreased from treatment with cardiac glycosides.[13] Owing to the involvement of Na^+/K^+-ATPase in numerous cellular functions, changing the chemical structures of cardiac glycosides to alter downstream signaling might be one strategy to repurpose this class of molecules for cancer treatment.

To date, several cardiac glycosides have been reported to exhibit cytotoxicity toward human cancer cells.[14] *Streblus asper* Lour. (Moraceae) is a small tree found in tropical countries inclusive of India, Sri Lanka, Malaysia, Thailand, and Vietnam. Various parts of this plant have been used in Ayurvedic medicine for the treatment of cardiac disorders, epilepsy, and edema.[15] (+)-Strebloside has been isolated and identified in our laboratories from two different collections of *S. asper* previously. From an initial sample of this plant collected in Thailand, (+)-strebloside showed potent cytotoxicity against HT-29 colon cancer and KB nasopharyngeal cells.[15] This compound was also obtained from a Vietnamese specimen of *S. asper*, and found to show significant potency in vivo against OVCAR3 ovarian and MDA-MB-231 breast cancer cells in a hollow fiber assay.[16]

In order to determine if (+)-strebloside can exert unique signaling among cardiac glycosides to induce cytotoxicity, it was compared to digitoxin in several cancer cell lines. In the current study, high-grade serous ovarian cancer cell lines were used. The results showed strebloside binds to Na^+/K^+-ATPase and further affects the cell cycle, cell proliferation, and induces apoptosis in ovarian cancer cells. Moreover, (+)-strebloside displayed similar signal transduction pathways to digitoxin. Activation of cell death by (+)-strebloside appears to be mediated through the Na^+/K^+-ATPase and its downstream signaling, and its anticancer activity mimics that of other cardiac glycosides.

RESULTS AND DISCUSSION

Na^+/K^+-ATPase Inhibition by (+)-Strebloside

The chemical structure of strebloside (Figure 1A) is similar to that of other cardiac glycosides, such as digitoxin (Figure 1A), digoxin, and ouabain, although it possesses a relatively unusual formyl group at C-10. Therefore, (+)- strebloside was tested for its ability to inhibit Na^+/K^+-ATPase activity. The cellular enzyme adenosine 5′-triphosphatase from the porcine cerebral cortex was incubated with various concentrations of (+)-strebloside, and digitoxin was used as positive control. (+)-Strebloside inhibited Na^+/K^+-ATPase activity in a concentration-dependent manner (Figure 1B). Like other cardiac glycosides, (+)-strebloside not only resembles a cardiac glycoside based on its chemical structure, but it also blocks the Na^+/K^+-ATPase pump.

Molecular Modeling of the Interactions of (+)-Strebloside and Digitoxin on Na^+/K^+-ATPase

A computer-simulated docking analysis was performed to compare (+)-strebloside and digitoxin in terms of their docking with Na^+/K^+-ATPase. The binding mode for these two compounds to this target was similar from the overlapping of the two docking complexes (Figures 1C-1E), with HO-14 forming an H-bond with T797. In addition, CHO-10 in (+)-strebloside forms an H-bond with Q111, while HO-3'a in the glycosyl portion of digitoxin forms an H-bond with the side-chain of R880. Van der Waal's force interactions were apparent between F786, L793, and the steroidal component of these two compounds, in addition to interactions of their respective lactone moieties between L125, A323, and T797.

(+)-Strebloside Inhibits Cell Proliferation

Cardiac glycosides that inhibit the Na^+/K^+-ATPase can also reduce cell viability. (+)-Strebloside showed significant cytotoxic activity against three different cancer cell lines as shown in Table 1. To analyze the activity of (+)-strebloside in high-grade serous ovarian cancer cells, several additional lines were used, including OVCAR3, OVSAHO, Kuramochi, OVCAR4, OVCAR5, and OVCAR8. (+)-Strebloside was active for all cell lines tested (Table 2), although it was somewhat less potent for Kuromachi cells. Comparative data for digitoxin are provided in Tables 1 and 2. Ovarian cancer is a heterogeneous disease, and the recent Cancer Genome Atlas Network analysis defined the deregulated pathways characterizing HGSC.[17] Different mutational gene spectrum of the cell lines might contribute the different response to (+)-strebloside and digitoxin.

To determine whether this cytotoxic action is specific to cancer cells, the IOSE-80 ovarian surface epithelial cell line, which expresses SV40 large T antigen, was treated with (+)-strebloside and digitoxin. These two cardiac glycosides were more potent in the normal immortalized cell line as compared to the tumor cell lines, consistent with previous reports in normal breast epithelial cells (MCF10A) and breast cancer cells[18] (Table 3). One reason that cardiac glycosides have continued to be pursued for anticancer activity is due to their efficacy in murine xenograft models. However, this has been suggested to be due to the ability of these compounds to selectively kill human cells as compared to murine cells due to differential expression in Na^+/K^+-ATPase. In support of these previous results, after three days of (+)- strebloside and digitoxin treatment, the growth of human cancer cells was inhibited, while murine oviductal epithelial cells (MOE) were not inhibited (Table 3). An MOE cells with silenced PTEN and activated KRAS, which was sufficient to drive tumorigenesis,[19] was not growth inhibited by either cardiac glycoside (Table 3). Thus, murine cells are more resistant than human cells to the antiproliferative effects of these cardiac glycosides. Despite being active in human cancer cells, the selective antitumor activity of cardiac glycosides in rodent models is probably due to species selective toxicity.

Cardiac glycosides possess multiple anticancer activities. There are four isoforms of the α subunit of Na^+/K^+-ATPase, namely, α1, α2, α3, and α4. The expression level of α1/3 subunits of Na^+/K^+-ATPase correlates with the susceptibility of cancer cells toward cardiac glycosides. Cancer cells with a higher ratio of the α3 to α1 isoform are more sensitive to cardiac glycoside treatment. The relative lack of α3 in some human tumor cells and rodent cells may explain their non-responsiveness to cardiac glycosides.[20] In fact, differences in the

isoforms of Na^+/K^+-ATPase located between normal and malignant cells determine its binding capability.[21] The data obtained in the present study demonstrate that murine cells are more resistant to cardiac glycosides than human cells, regardless of whether they were considered normal or malignant. Notably, (+)-strebloside and digitoxin show different cytotoxicity in HGSC and normal cells, with normal cells being more susceptible. Similarly, MCF10A cells are more susceptible than MCF7 cells to digitoxin.[18] However, as reported by Ren et al., (+)-strebloside was not as toxic as digoxin in normal human colon CCD-112CoN cells and normal human peripheral blood mononuclear cells.[16]

To further assess the antiproliferative phenotype of (+)-strebloside, OVCAR3 and OVSAHO cells were used to evaluate cytotoxic activity. A clonogenic assay was employed to monitor the ability of (+)-strebloside treated cells to form colonies as compared to control. The cells were treated with drug or solvent control every three days for the entire assay. The negative control group formed a significant number of colonies after 21 days, while neither OVCAR3 nor OVSAHO cells formed colonies when exposed to (+)-strebloside (Figures 2A and 2B). Next, the cells were grown in soft agar to test whether (+)-strebloside inhibited anchorage-independent growth. (+)-Strebloside-treated cells formed significantly less soft agar colonies than a DMSO control using OVCAR3 cells, while no difference was detected with OVSAHO cells (Figures 2C and 2D).

(+)-Strebloside Blocks the Cell Cycle

To investigate if cells undergo cell cycle arrest as a consequence of (+)-strebloside treatment, cells treated with this compound were collected and subjected to flow cytometry after propidium iodide staining. Figure 3A shows that (+)-strebloside induced an accumulation of cells in the G2/M phase of the OVCAR3 cell cycle, similar to cells treated with digitoxin (Figure 3B). Next, the cyclin dependent kinase inhibitor p21 was measured using western blot as marker of cell cycle arrest. Quantitative densitometry confirmed that (+)-strebloside- and digitoxin-treated cells expressed more p21 protein than the control (Figures 3C and 3D). Similar results were observed in OVSAHO cells (Figure S1, Supporting Information). OVCAR3 and OVSAHO cells treated with either (+)-strebloside or digitoxin both demonstrated a significant increase in p21 expression, suggesting p21 enhances the blockage of the cell cycle.

(+)-Strebloside Induces Apoptosis

To determine the mechanism of cardiac glycoside-induced cytotoxicity, western blot analyses were performed. As shown in Figure 4A, treatment of OVCAR3 cells with either (+)-strebloside or digitoxin led to a significant increase in cleaved caspase 3 as well as its downstream target, cleaved PARP. Quantitative densitometry was performed using OVCAR3 cells. Cells exposed to either (+)-strebloside or digitoxin expressed significantly higher levels of cleaved PARP and cleaved caspase 3 when compared to control cells (Figures 4B and 4C). There was a decrease in the antiapoptotic protein Mcl-1 and Bcl-xL after either (+)-strebloside or digitoxin treatment (Figures 4D and 4E). Quantitative densitometry confirmed that (+)-strebloside- or digitoxin-treated cells expressed less Mcl-1 than control cells (Figures 4F). The decrease in Bcl-xL after treatment was not statistically significant (Figures 4G). Next, western blotting and quantitative densitometry were performed on OVSAHO

cells exposed to either (+)-strebloside or digitoxin. Cleaved PARP expression levels in (+)-strebloside- or digitoxin- treated cells were higher than the levels in control cells (Figures S2A and S2B, Supporting Information). These results suggest that the apoptotic effect of (+)-strebloside in OVCAR3 cells is mediated by the increase of cleaved caspase 3, cleaved PARP, and suppression of Mcl-1.

The altered expression of the antiapoptotic Bcl-2 protein family is a common pattern in cancer.[22] Most cancer cell models overexpress one or more of the three major proteins: Bcl-2, Bcl-xL, and Mcl-1. Mcl-1 repression occurs in different cancer cell models after treatment with cardiac glycosides. Cardenolides (digoxin, digitoxin, ouabain) or bufadienolides (cinobyfagin and proscillaridin) all have been reported to downregulate Mcl-1.[23] (+)-Strebloside also resulted in Mcl-1 downregulation to activate apoptosis.

Decrease of Mutant p53 Expression by (+)-Strebloside is ERK Pathway Dependent

In order to reveal some of the pathways that might be modified by (+)-strebloside, western blots of OVCAR3 and OVSAHO lysates were performed, and the results were compared to digitoxin as a positive control. Given the high percentage of p53 mutation in HGSC, p53 has been a central target for mechanism-driven cancer drug discovery. Furthermore, it has been reported that the cardiac glycosides digoxin and ouabain reduce p53 protein levels.[24] Since most of these studies were done with cells that express either wild-type or mutant p53, and high grade serous ovarian cancer cells should all express mutant p53, the ability of (+)-strebloside to reduce p53 protein levels was examined. Treatment of (+)-strebloside and digitoxin resulted in the disappearance of p53 (Figures 5A and 5B). Since p53 expression was not detectable in OVSAHO cells, OVCA432 cells were treated with (+)-strebloside or digitoxin, which resulted in decreased expression of p53 (Figures S3A and S3B, Supporting Information). In addition, inhibition of Na^+/K^+-ATPase can transduce intracellular signals via multiple pathways, including mitogen-activated protein kinases (MAPK). Previous reports demonstrated that a MAPK inhibitor was able to block cardiac glycoside-induced repression of p53.[24] Extracellular signal-regulated kinases (ERKs) are members of MAPK. Phosphorylated ERK and total ERK were probed in response to (+)-strebloside and digitoxin treatment. Both cell lines showed induced activation of ERK after treatment with (+)-strebloside (Figures 5C and 5D) or digitoxin (Figures 5E and 5F). These data are consistent with previous reports where cardiac glycoside-induced cell death was mediated by activation of ERK, followed by the decreases in p53. Overall, these findings suggest the MAPK pathway is downstream of Na^+/K^+ ATPase and contributes to decreased mutant p53 expression in HGSC cells.

The p53 tumor suppressor protein is a transcription factor that controls many cellular functions such as DNA repair, cell cycle, and apoptosis. It is the most commonly mutated gene in all human cancers.[25] Approaches are currently under investigation to target p53 and its regulators, including gene therapy to restore p53 function, inhibition of MDM2, refolding of mutant p53 to wild-type p53, eliminating mutant p53, and targeting p53 family proteins like p63 and p73.[26, 27] Some of these p53-targeted therapies have entered clinical trials.[26, 28] A recent study suggests that digoxin and ouabain reduced mutant p53 level through MAPK signaling pathways, initiated through the inhibition of Na^+/K^+-ATPase.[24] Remarkably, (+)-

strebloside and digitoxin induce ERK phosphorylation and down-regulation of mutant p53 in ovarian cancer cells, indicating a common effect of these two cardiac glycosides. Since cardiac glycosides seem to also harm normal cells and despite structural differences they all similarly modify Na^+/K^+-ATPase, the ability to use them for targeting p53 is unlikely to be able to avoid these alternative deleterious problems.

(+)-Strebloside Inhibits NF-κB Transcription Activity

Cardiac glycosides have also been shown to inhibit cell survival by inhibiting NF-κB signaling. To further characterize how (+)-strebloside modulates signal transduction pathways that may contribute to their ability to hinder tumor growth, a luciferase assay was employed that quantifies regulation of the NF-κB promoter. OVCAR3 cells were transfected with an NF-κB reporter gene and exposed to (+)-strebloside or digitoxin. When cells were incubated with TNF-α, activation in NF-κB reporter activity was observed. By contrast, TNF-α co-treated with (+)-strebloside or digitoxin decreased NF-κB signaling 29% and 50%, respectively (Figures 6A and 6B). Collectively, these findings, suggest (+)-strebloside shares common features of other cardiac glycosides, which are reported to inhibit NF-κB signaling.[29]

The NF-κB transcription factors are expressed in many tissue types in processes related to growth, differentiation, and inflammation. Constitutive NF-κB signaling also has been identified in tumors of epithelial origin including breast, colon, lung, and ovarian carcinomas.[30] Recent work suggested NF-κB conveyed poor outcomes in ovarian cancer.[31] Cardiac glycosides potently induce mitotic arrest through downregulation of the nuclear transcription factor, NF-κB.[32] Consistent with this finding, (+)-strebloside induced G2/M phase arrest and inhibition of NF-κB activity. These findings suggest cardiac glycosides may also be useful in targeting the pro-inflammatory component responsible for cancers. Despite the structural differences between (+)-strebloside and digitoxin, similar downstream signals appear to arise from both compounds in both normal and cancer cells.

Electrophysiological Characterization of (+)-Strebloside

Many drugs cause side effects that can upset the balance between benefit and risk of a specific therapy. One of the most important adverse effects of drugs involve prolongation of the cardiac action potential (acquired long QT syndrome; aLQT2), which is caused mostly by inhibition of the human *ether-a-go-go* related gene (hERG) potassium channels and can be associated with ventricular fibrillation and sudden death. Several drugs have been removed from the market or have received restrictive labeling because of their association with aLQT2. The present electrophysiological study revealed that (+)-strebloside did not exert any change on any of the hERG1 biophysical parameters that were measured including peak current amplitude, current-voltage relationship, and voltage-dependence of current deactivation and activation (Figure 7). These data suggest that (+)-strebloside is neither a hERG1 blocker nor activator and that it should not cause aLQT2 if it were to be used in clinical practice. In contrast, digitoxin has been reported to interact with hERG channels and hERG trafficking.[33, 34]

Cardiac glycosides are clinically used for the treatment of heart failure and atrial arrhythmia. (+)-Strebloside was isolated from *Streblus asper*[15,16] and possesses a common cardiac glycoside structure, yet few studies have focused on its potential cardiac glycoside activity. In this part of the investigation, we contemplated whether (+)-strebloside may also exhibit anticancer action in ovarian cancer cells, in comparison to digitoxin, one of the most commonly prescribed cardiac glycosides. In vivo hollow fiber assay results have shown that (+)-strebloside inhibited MDA-MB-231 and OVCAR3 cell growth.[16] As mentioned earlier, an ATPase assay and molecular modeling also demonstrated that (+)-strebloside binds Na^+/K^+-ATPase. (+)-Strebloside increased p21, a marker of cell cycle progression, and increased the percentage of cells in the G2/M phase of the cell cycle. In addition, (+)-strebloside-treated cells showed apoptosis features such as increased cleaved caspase 3 and cleaved PARP protein levels and decreased Mcl-1. Consistent with other cardiac glycosides, (+)-strebloside activated ERK and decreased mutant p53. Furthermore, (+)-strebloside inhibited NF-κB transcription activity. Thus, (+)-strebloside could be a potential anticancer drug candidate, if it exhibited better anticancer properties than digitoxin.

In conclusion, both (+)-strebloside and digitoxin share a Na^+/K^+-ATPase binding mode based on an in vitro bioassay and molecular docking and inhibition. Similar to digitoxin, (+)-strebloside downregulated antiapoptotic proteins such as Mcl-1 and induced apoptosis, by initiating caspase signaling and PARP cleavage. The inhibition of Na^+/K^+-ATPase by (+)-strebloside was found to affect the mitotic cell cycle, proliferation, repression of p53, and NF-κB. However, treatment with (+)-strebloside did not appear vastly different from digitoxin, which has displayed mixed results for breast and ovarian cancers based on epidemiological studies of women consuming these compounds long-term for treatment of cardiovascular disease. This study demonstrates that the key signaling events induced by (+)-strebloside are highly similar to other more well-known cardiac glycosides, and therefore this compound could likely suffer from the same side effects. Antibody-drug conjugates (ADCs) that enhance the selective targeting of cancer cells could maximize the cardiac glycoside efficacy, while reducing their system side effect by preventing nonspecific uptake by normal cells. Further chemical alteration of cardiac glycosides might help to reduce negative side effects while increasing cancer cell cytotoxicity.

EXPERIMENTAL SECTION

Test Compounds

(+)-Strebloside was isolated in pure form and characterized from the stem bark of *Streblus asper*, as described previously.[16] Digitoxin was purchased from Sigma-Aldrich Corp. (St. Louis, MO, USA).

Cell Culture

MDA-MB-435 human melanoma cancer cells, MDA-MB-231 human breast cancer cells, HT-29 human colon cancer cells, and OVCAR3 human ovarian cancer cells were purchased from the American Type Culture Collection (Manassas, VA, USA). Cells were propagated in RPMI 1640 medium supplemented with 10% fetal bovine serum, and 1% penicillin/streptomycin. OVSAHO and Kuramochi cells obtained from the Japanese Collection of

Research Bioresources Cell Bank (JCRB) were grown in RPMI 1640 with 10% fetal bovine serum, and 1 × penicillin/streptomycin. OVCAR4 cells were obtained from the National Cancer Institute from the Division of Cancer Treatment and Diagnosis Tumor Repository and were grown in RPMI 1640 with 10% fetal bovine serum, 1% L-glutamine, and 1% penicillin/streptomycin. OVCA 432 (gifts from Dr. Gustavo Rodriguez and Dr. Teresa Woodruff at Northwestern University) and OVCAR5 cells (Developmental Therapeutics Program at National Cancer Institute) were maintained in Minimum Essential Medium (MEM) supplemented with 10% fetal bovine serum (FBS), 1% L-glutamine, 1% non-essential amino acids, 1% sodium pyruvate, and 1% penicillin/streptomycin. OVCAR8 cells were obtained from ATCC and grown in DMEM with 10% fetal bovine serum, and 1% penicillin/streptomycin. Normal immortalized human ovarian surface epithelial cells (IOSE 80) were a gift from Dr. Nelly Auersperg at the University of Vancouver and were maintained in 50% v/v Medium 199 and 50% v/v MCDB (Sigma-Aldrich, St. Louis, MO, USA), 15% FBS, 1% L-glutamine, 1% penicillin/streptomycin, and 0.055% epithelial growth factor (EGF) (PeproTech, Inc., Rocky Hill, NJ, USA). Cultured cells were maintained at 37 °C in 5% CO_2.

Primary murine oviductal epithelial (MOE) cells (also called murine tubal epithelial cells or MTEC) were pooled from multiple oviducts to establish one cell line from 8-week-old female CD1 mice, as previously described.[35] Once the primary isolated MOE cells became established in culture, the MOE^{LOW} cells (passages 8–25) were continuously passaged to generate the experimentally aged, MOE^{HIGH} cells (passages 85–120). MOE cells were maintained in complete medium containing α-MEM modified Eagle's medium (CellGro, Manassas, VA, USA) supplemented with ribonucleosides, deoxynucleosides, L-glutamine, 10% fetal bovine serum, 2 mM L-glutamine (Life Technologies, Grand Island, NY, USA), 2 μg/mL epithelial growth factor, 5 μg/mL insulin, 5 μg/mL transferrin, 5 ng/mL sodium selenite (Roche, Indianapolis, IN, USA), 1 mg/mL gentamycin (CellGro, Manassas, VA, USA), and 18.2 μg/mL β-estradiol (Sigma Aldrich). MOE scrambled cells and MOE $PTEN^{shRNA}/KRAS^{G12V}$ stable clones were generated from MOE cells obtained from Dr. Barbara Vanderhyden at the University of Ottawa. MOE scrambled cells were maintained in MOE medium containing 0.5 μg/mL puromycin and MOE $PTEN^{shRNA}/KRAS^{G12V}$ cells were maintained in MOE medium containing 0.5 μg/mL puromycin and 200 μg/mL hygromycin. MOE cells were maintained in a humidified atmosphere containing 5% CO_2 at 37 °C.

Cell Viability Assay

Cells in log phase growth were harvested by trypsinization followed by two PBS washings to remove all traces of enzyme. Cells were seeded at 5,000 cells per well in 96-well clear, flat-bottomed plates and incubated overnight. (+)-Strebloside or digitoxin dissolved in DMSO was diluted and added to the appropriate wells. The cells were incubated for 72 h and evaluated for viability with a commercial absorbance assay (CellTiter 96® AQueous One Solution Cell Proliferation Assay; Promega, Madison, WI, USA) that measured viable cells. IC_{50} values were determined in nM relative to the solvent (DMSO) control.

Cell Cycle Assay

Cells were plated in 6-well plates and treated with vehicle, (+)-strebloside or digitoxin for 72 h. After treatment, the cells were collected by trypsinization, fixed in 70% ethanol, washed in PBS, resuspended in 1 mL of PBS containing 1 mg/mL RNase and 50 μg/mL propidium iodide, incubated in the dark for 30 min at room temperature, and analyzed using an EPICS flow cytometer (Beckman-Coulter; Brea, CA, USA). The data were analyzed using Multicycle software (Phoenix Flow Systems; San Diego, CA, USA).

Immunoblot Analysis

Whole cell lysates were prepared from OVCAR3, OVSAHO, or OVCA432 cells treated with (+)-strebloside or digitoxin. After treatment, cells were harvested, washed twice with PBS and re-suspended in RIPA Lysis and Extraction Buffer (Thermo Scientific, Rockford, IL, USA), and incubated on ice for 15 min. After centrifugation (4 °C, 15 min and 14,000 g) supernatants containing cellular proteins were collected. Protein concentration was determined by the BCA assay (Pierce, Rockford, IL, USA). Cell lysates were adjusted for protein content and equal amounts (25 μg) separated by SDS-PAGE. Proteins were immobilized onto PVDF membranes. After saturating with 5% (w/v) non-fat milk in TBST for 1 h at room temperature, the membranes were incubated with primary antibody overnight at 4 °C. The following primary antibodies were used: Actin 1:1000 (cat. no. A2066, Sigma-Aldrich, St. Louis, MO, USA); p53 1:500 (cat. no. SC6243, Santa Cruz Biotechnology, Dallas, TX, USA); p21 1:300 (cat no. 2947), PARP 1:500 (cat. no. 9542), caspase 3 1: 300 (cat. no. 9662), Mcl-1 1: 500 (cat. no. 4572), Bcl-xL 1: 500 (cat. no. 2764), phosphor-ERK 1:500 (cat. no. 4370), ERK 1:500 (cat. no. 4695) (Cell Signaling, Beverly, MA, USA). Anti-rabbit HRP-linked secondary antibodies (Cell Signaling Technology, Inc.) were used at a concentration of 1:1000 for all blots except for actin, which was used at 1: 10,000 (Promega, Madison, WI, USA) for 30 min in blocking buffer. After washing, membranes were incubated in SuperSignal West Femto substrate (Thermo Scientific), before imaging on a FlourChem™ E system (ProteinSimple, Santa Clara, CA, USA). Densitometric analysis was performed using NIH ImageJ.

Na^+/K^+-ATPase Activity Assay

Na^+/K^+-ATPase activity was assessed using a luminescent ADP detection assay (ADP-Glo Max Assay; Promega) that measures enzymatic activity by quantitating the ADP produced during the enzymatic first half-reaction. Specifically, 10 μL of assay buffer containing adenosine 5′-triphosphatase (ATP) from Porcine Cerebral Cortex (Sigma) were added to the wells of a 96-well plate followed by 10 μL of DMSO or DMSO containing (+)-strebloside or digitoxin. Then, each well received 5.0 μL of ATP to initiate the reaction. Final assay concentrations contained different concentration of (+)-strebloside or digitoxin. After 15 min incubation at 37 °C, 25 μL ADP-Glo Reagent were added to terminate the reaction, and plates were incubated at room temperature for 40 min to deplete the remaining ATP. Next, 50 μL of Kinase Detection Reagent was added, and plates were incubated for 60 min at room temperature to convert ADP to ATP. ATP was measured via a luciferin/luciferase reaction using a Synergy Mx (BioTek, Winooski, VT, USA) to assess luminescence.

Molecular Modeling

The crystal structure of Na^+/K^+-ATPase when complexed with digoxin (PDB code 4ret) was optimized using the Protein Preparation Wizard (Schrödinger, LLC, New York, NY). Restrained minimization was performed on hydrogen atoms in the OPLS3 force field. The 3D structures of digitoxin and (+)-strebloside were prepared using LigPrep (Schrödinger, LLC, New York, NY). The OPLS3 force field was used for ligand geometric optimization with neutralized ionization and the chiralities were assigned based on their natural structures. Default values were used for other parameters during protein and ligand preparations. The following molecular dockings were performed using the GOLD v5.2.2[36] with the above-prepared protein and ligands. The active site for the enzyme was defined within 10 Å around the catalytic site of (−28.6, −19.8, 70.9) in the crystal structure. Scaffold constraints with tetracyclic steroidal rings were used for the docking pose prediction. The best scoring pose for each compound was extracted for further analysis. Illustrations were made using Chimera.[37]

Electrophysiological Recordings and Analysis

Potassium currents were recorded under voltage-clamp with an EPC10 patch clamp amplifier interface (HEKA Electronics, Lambrecht, Pfalz, Germany). For data acquisition, pulse generation, and analysis, a computer (Dell, Round Rock, TX, USA) running PULSE software (HEKA Electronics) was used. All experiments were conducted at room temperature (20–24 °C). Data are presented as means ± SE of three experiments. The patch pipettes were made from Corning type 7052 glass (Garner Glass, Claremont, CA, USA). Whole-cell currents were obtained conventionally from dialyzed cells voltage-clamped through ruptured membrane patches. The solution bathing the cells contained: 140 mM NaCl, 10 mM HEPES, 1 mM $CaCl_2$, 1 mM $MgCl_2$, 5 mM KCl, and 10 mM glucose, having the pH adjusted to 7.4 saline, and was superfused at 1 mL/min. The pipette solution contained 140 mM KCl, 2 mM $MgCl_2$, 1 mM $CaCl_2$, 10 mM HEPES, and 2.5 mM EGTA (~50 nM free Ca^{2+}), with the pH adjusted to 7.2. The pulse protocol was run a minimum of 10 times before the perfusion with (+)-strebloside to ensure that the currents were stable.

Clonogenic Assay

OVCAR3 and OVSAHO cells were plated (200 cells/60 mm-dish) and incubated for 21 days. After incubation, cells were washed, fixed with 4% (w/v) paraformaldehyde, and stained with 0.04% (w/v) crystal violet for 30 min at room temperature. Plates were washed with deionized H_2O, dried, and photographed using the FluorChem E documentation system (Protein Simple, Santa Clara, CA, USA). Numbers of foci were analyzed using Image J software[16] from three biological replicates.

Soft Agar Colony Formation Assay

OVCAR3 and OVSAHO cells were suspended (1.5×10^4) in 0.35% w/v agar on top of a 0.5% w/v base agar layer. Cells were incubated for 21 days, with the medium changed every three days. Final colonies were imaged on a Nikon Eclipse TS100 microscope and colonies were counted using Image J software from three biological replicates.

Luciferase Assay

Cells were plated at a density of 25,000 per well into 24-well plates and incubated overnight. Cells were transfected with 0.05 μg/well of an expression construct containing the NF-κB binding element promoter upstream of the luciferase gene using Mirus TransIT LT1 (Mirus Bio LLC, Madison, WI, USA), according to the manufacturer's instructions. Cells were transfected for 24 h in serum-supplemented medium. Cells were then treated with TNFα at 10 ng/mL (Sigma Aldrich), and (+)-strebloside (100 nM) or digitoxin (100 nM) for 4 h. Normal cell luciferase activity was measured using a Synergy Mx (BioTek).

Statistical Analysis

Each experiment was replicated at least three times and data is presented as mean ± SEM. Data were analyzed by a paired T-test, or ANOVA followed by Dunnett's or Kruskal-Wallis post hoc analysis. A p value of ≤ 0.05 was considered significant. Analysis was carried out with PRISM version 6.0b.

Supplementary Material

Refer to Web version on PubMed Central for supplementary material.

Acknowledgments

This investigation was supported by grant P01 CA125066 funded by the National Cancer Institute, NIH, Bethesda, MD.

References

1. Stenkvist B, Bengtsson E, Eriksson O, Holmquist J, Nordin B, Westman-Naeser S. Lancet. 1979; 1:563. [PubMed: 85158]
2. Haux J, Klepp O, Spigset O, Tretli S. BMC Cancer. 2001; 1:11. [PubMed: 11532201]
3. Platz EA, Yegnasubramanian S, Liu JO, Chong CR, Shim JS, Kenfield SA, Stampfer MJ, Willett WC, Giovannucci E, Nelson WG. Cancer Discov. 2011; 1:68–77. [PubMed: 22140654]
4. Apostolou P, Toloudi M, Chatziioannou M, Ioannou E, Knocke DR, Nester J, Komiotis D, Papasotiriou I. BMC Pharmacol Toxicol. 2013; 14:18. [PubMed: 23521834]
5. Felth J, Rickardson L, Rosen J, Wickstrom M, Fryknas M, Lindskog M, Bohlin L, Gullbo J. J Nat Prod. 2009; 72:1969–1974. [PubMed: 19894733]
6. Babula P, Masarik M, Adam V, Provaznik I, Kizek R. Anticancer Agents Med Chem. 2013; 13:1069–1087. [PubMed: 23537048]
7. Vogel TJ, Jeon C, Karlan B, Walsh C. Gynecol Oncol. 2016; 140:285–288. [PubMed: 26691221]
8. Takai N, Ueda T, Nishida M, Nasu K, Narahara H. Int J Mol Med. 2008; 21:637–643. [PubMed: 18425357]
9. Prassas I, Diamandis EP. Nat Rev Drug Discov. 2008; 7:926–935. [PubMed: 18948999]
10. Xie Z, Cai T. Mol Interv. 2003; 3:157–168. [PubMed: 14993422]
11. Haas M, Wang H, Tian J, Xie Z. J Biol Chem. 2002; 277:18694–18702. [PubMed: 11907028]
12. Aydemir-Koksoy A, Abramowitz J, Allen JC. J Biol Chem. 2001; 276:46605–46611. [PubMed: 11579090]
13. Xu Z, Wang F, Fan F, Gu Y, Shan N, Meng X, Cheng S, Liu Y, Wang C, Song Y, Xu R. J Proteome Res. 2015; 14:4594–4602. [PubMed: 26491887]
14. Wang TM, Hojo T, Ran FX, Wang RF, Wang RQ, Chen HB, Cui JR, Shang MY, Cai SQ. J Nat Prod. 2007; 70:1429–1433. [PubMed: 17844995]

15. Rastogi S, Kulshreshtha DK, Rawat AK. Evid-Based Complement Alternat Med. 2006; 3:217–222. [PubMed: 16786051]
16. Ren Y, Chen WL, Lanvit DD, Sass EJ, Shriwas P, Nihn TN, Chai HB, Zhang X, Soejarto DD, Chen X, Lucas DM, Swanson SM, Burdette JE, Kinghorn AD. J Nat Prod. 2017; 80 In press.
17. Cancer Genome Atlas Research. Nature. 2011; 474:609–615. [PubMed: 21720365]
18. Clifford RJ, Kaplan JH. PLoS One. 2013; 8:e84306. [PubMed: 24349570]
19. Eddie SL, Quartuccio SM, E OH, Moyle-Heyrman G, Lantvit DD, Wei JJ, Vanderhyden BC, Burdette JE. Oncotarget. 2015; 6:20500–20512. [PubMed: 25971410]
20. Yang P, Menter DG, Cartwright C, Chan D, Dixon S, Suraokar M, Mendoza G, Llansa N, Newman RA. Mol Cancer Ther. 2009; 8:2319–2328. [PubMed: 19671733]
21. Yang P, Cartwright C, Efuet E, Hamilton SR, Wistuba II, Menter D, Addington C, Shureiqi I, Newman RA. Mol Carcinog. 2014; 53:253–263. [PubMed: 23073998]
22. Juin P, Geneste O, Gautier F, Depil S, Campone M. Nat Rev Cancer. 2013; 13:455–465. [PubMed: 23783119]
23. Cerella C, Muller F, Gaigneaux A, Radogna F, Viry E, Chateauvieux S, Dicato M, Diederich M. Cell Death Dis. 2015; 6:e1782. [PubMed: 26068790]
24. Wang Z, Zheng M, Li Z, Li R, Jia L, Xiong X, Southall N, Wang S, Xia M, Austin CP, Zheng W, Xie Z, Sun Y. Cancer Res. 2009; 69:6556–6564. [PubMed: 19679550]
25. Kandoth C, McLellan MD, Vandin F, Ye K, Niu B, Lu C, Xie M, Zhang Q, McMichael JF, Wyczalkowski MA, Leiserson MD, Miller CA, Welch JS, Walter MJ, Wendl MC, Ley TJ, Wilson RK, Raphael BJ, Ding L. Nature. 2013; 502:333–339. [PubMed: 24132290]
26. Wang Z, Sun Y. Transl Oncol. 2010; 3:1–12. [PubMed: 20165689]
27. Yu X, Narayanan S, Vazquez A, Carpizo DR. Apoptosis. 2014; 19:1055–1068. [PubMed: 24756955]
28. Hong B, van den Heuvel AP, Prabhu VV, Zhang S, El-Deiry WS. Curr Drug Targets. 2014; 15:80–89. [PubMed: 24387333]
29. Yang Q, Huang W, Jozwik C, Lin Y, Glasman M, Caohuy H, Srivastava M, Esposito D, Gillette W, Hartley J, Pollard HB. Proc Natl Acad Sci USA. 2005; 102:9631–9636. [PubMed: 15983368]
30. Basseres DS, Baldwin AS. Oncogene. 2006; 25:6817–6830. [PubMed: 17072330]
31. Annunziata CM, Stavnes HT, Kleinberg L, Berner A, Hernandez LF, Birrer MJ, Steinberg SM, Davidson B, Kohn EC. Cancer. 2010; 116:3276–3284. [PubMed: 20564628]
32. Xie CM, Liu XY, Yu S, Cheng CH. Carcinogenesis. 2013; 34:1870–1880. [PubMed: 23615397]
33. Wang L, Wible BA, Wan X, Ficker E. J Pharmacol Exp Ther. 2007; 320:525–534. [PubMed: 17095614]
34. Wang L, Dennis AT, Trieu P, Charron F, Ethier N, Hebert TE, Wan X, Ficker E. Mol Pharmacol. 2009; 75:927–937. [PubMed: 19139152]
35. Quartuccio SM, Lantvit DD, Bosland MC, Burdette JE. PLoS One. 2013; 8:e65067. [PubMed: 23741457]
36. Verdonk ML, Cole JC, Hartshorn MJ, Murray CW, Taylor RD. Proteins. 2003; 52:609–623. [PubMed: 12910460]
37. Pettersen EF, Goddard TD, Huang CC, Couch GS, Greenblatt DM, Meng EC, Ferrin TE. J Comput Chem. 2004; 25:1605–1612. [PubMed: 15264254]

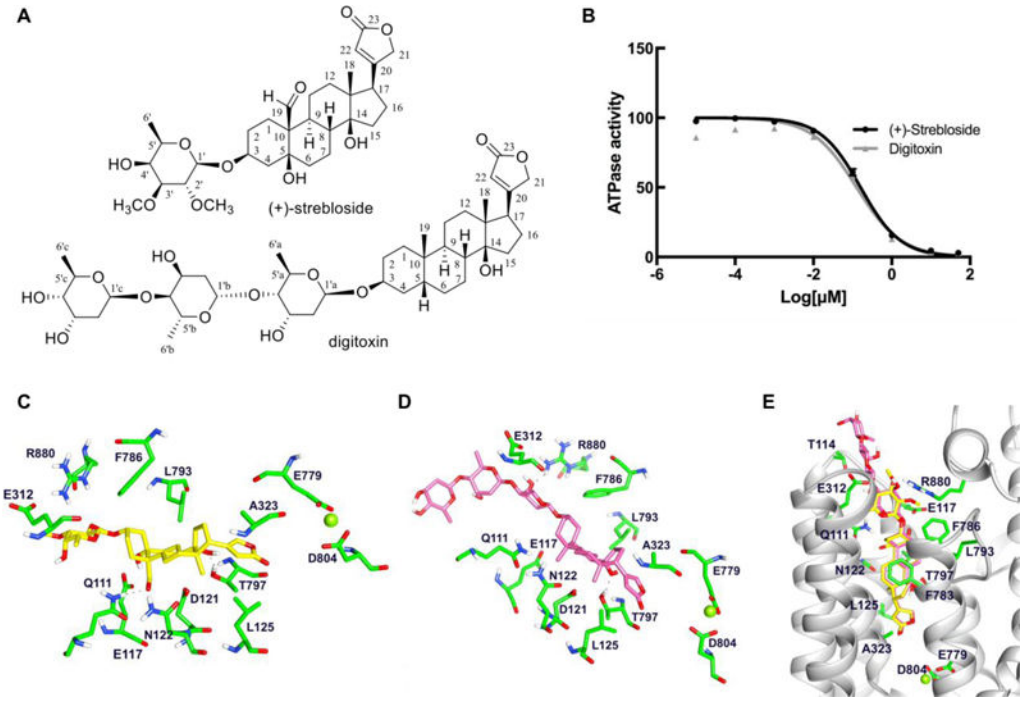

Figure 1.

(A) Structures of (+)-strebloside and digitoxin. (B) ATPase assay of Na^+/K^+-ATPase treated with (+)-strebloside and digitoxin, with activity determined and displayed as the percentage of activity relative to the untreated sample. (C-E) Binding of (+)-strebloside (yellow) and digitoxin (pink) to Na^+/K^+-ATPase as investigated by molecular modeling. (C) The predicted (+)-strebloside-binding mode. (+)-Strebloside and the amino acids in the active site are depicted by yellow and green sticks. OH-14 and CHO-10 of strebloside form H-bonds with the side-chains of T797 and Q111, respectively. (B) The predicted digitoxin-binding mode. Digitoxin and the amino acids in the binding cavity are depicted in pink and green sticks. HO-14 of digitoxin forms an H-bond with the side-chain of T797, and HO-3'a in the glycosyl part forms an H-bond with the side-chain of R880. The Mg^{2+} ion occupying cation site II is represented by a green sphere in panels C and D. (E) Overlapping the docking poses of (+)-strebloside and digitoxin. Digitoxin, (+)-strebloside and the amino acids in the binding cavity are depicted as pink, yellow and green sticks, respectively, and the Na^+/K^+-ATPase is shown as a gray ribbon.

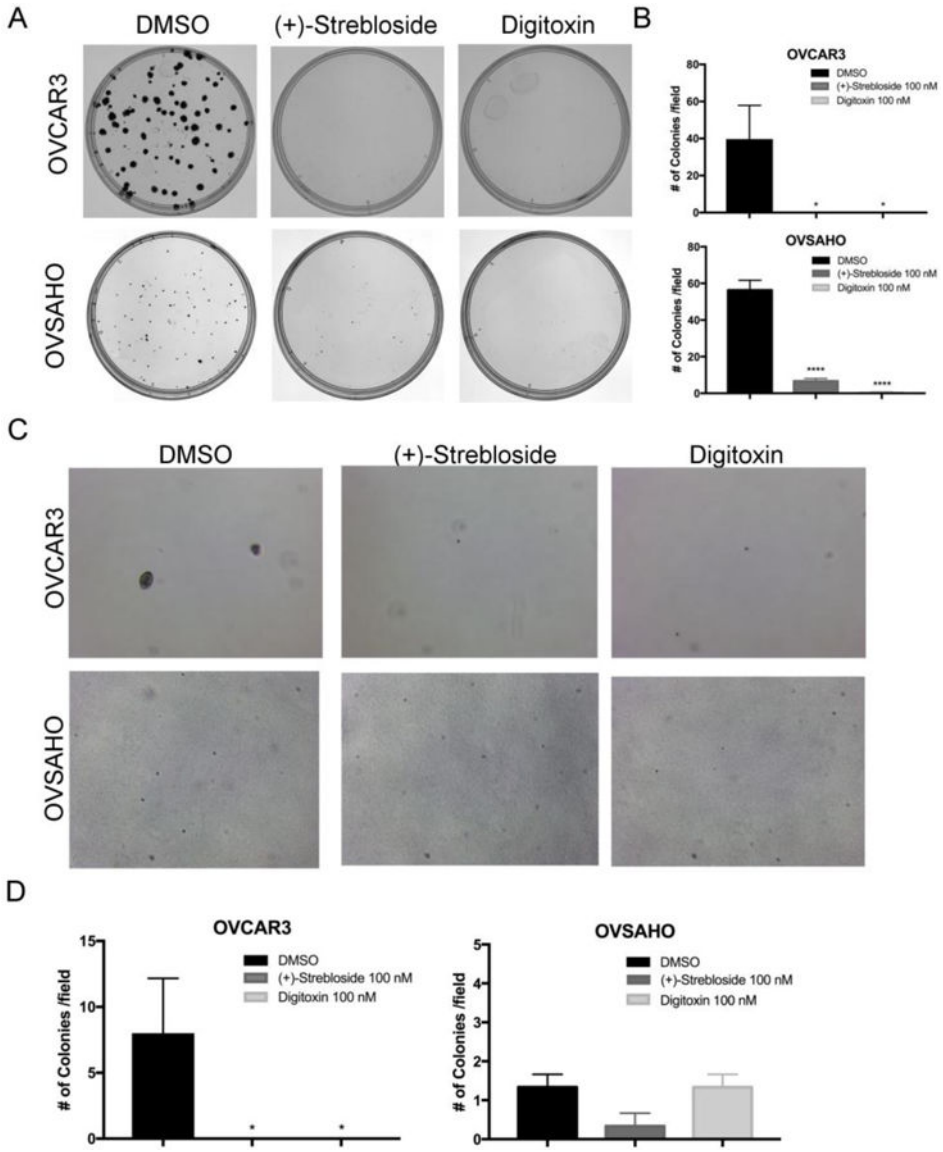

Figure 2.

(+)-Strebloside inhibits 2D colony formation and 3D soft agar colony growth. (A and B) OVCAR3 and OVSAHO cells were treated with (+)-strebloside and digitoxin then tested for 2D colony formation after 21 days using a clonogenic assay. (C and D) OVCAR3 and OVSAHO cells were treated with (+)-strebloside and digitoxin then analyzed for soft agar colony formation after 21 days (**** $p \leq 0.0001$).

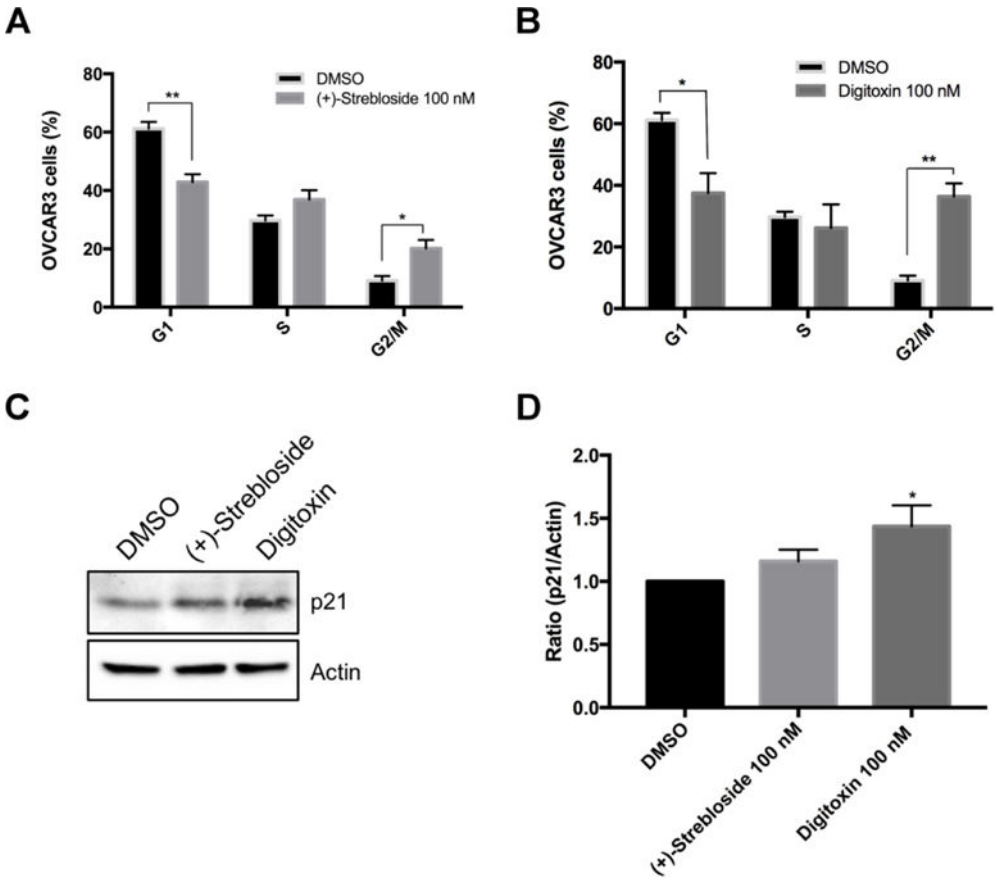

Figure 3.

(+)-Strebloside inhibits cell proliferation in OVCAR3 human ovarian cancer cells. (A and B) Cells were treated with DMSO, (+)-strebloside or digitoxin for 72 h prior to analysis by flow cytometry. Graphs displaying differences in cell cycle phases. (C) Western blot of OVCAR3 cell lysates treated with either (+)-strebloside or digitoxin were probed for p21 and actin. (D) Quantitative densitometry of western blots indicate increase expression of p21 in OVCAR3 cells ($n = 3$). Data represented as means ± SEM (* $p \leq 0.05$, ** $p \leq 0.01$).

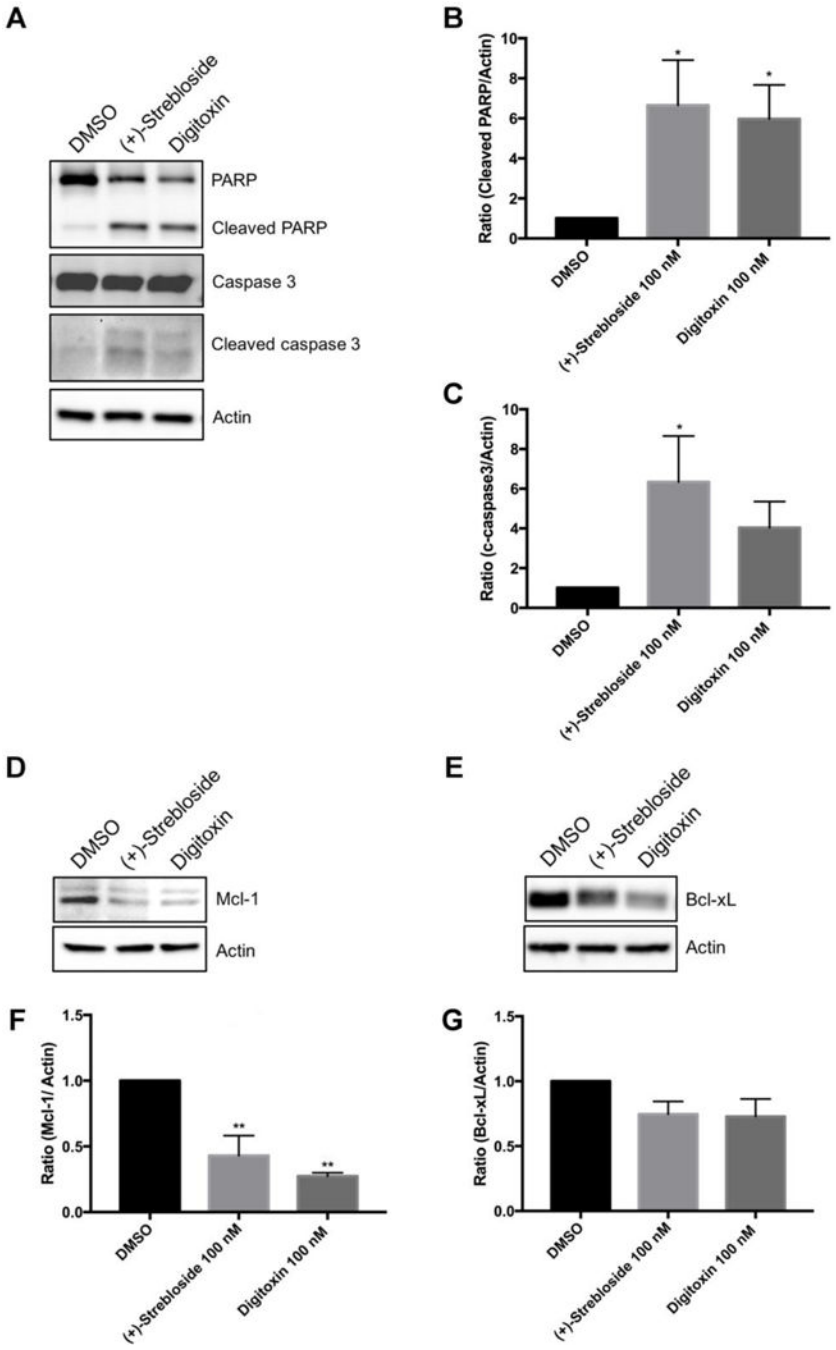

Figure 4.

(+)-Strebloside induces apoptosis in OVCAR3 cells. (A) Western blot of OVCAR3 cell lysates treated with (+)-strebloside and digitoxin were probed for PARP, caspase 3, cleaved caspase3, and actin. (B and C) Quantitative densitometry of western blots indicated increased expression of cleaved PARP and cleaved caspase 3 in OVCAR3 cells ($n = 3$). (D and E) Western blotting of OVCAR3 cell lysates treated with (+)-strebloside or digitoxin were probed for Mcl-1, Bcl-xL and actin. (F and G) Quantitative densitometry of western blots indicated decreased expression of Mcl-1 OVCAR3 cells ($n = 3$. * $p \leq 0.05$, ** $p \leq 0.01$).

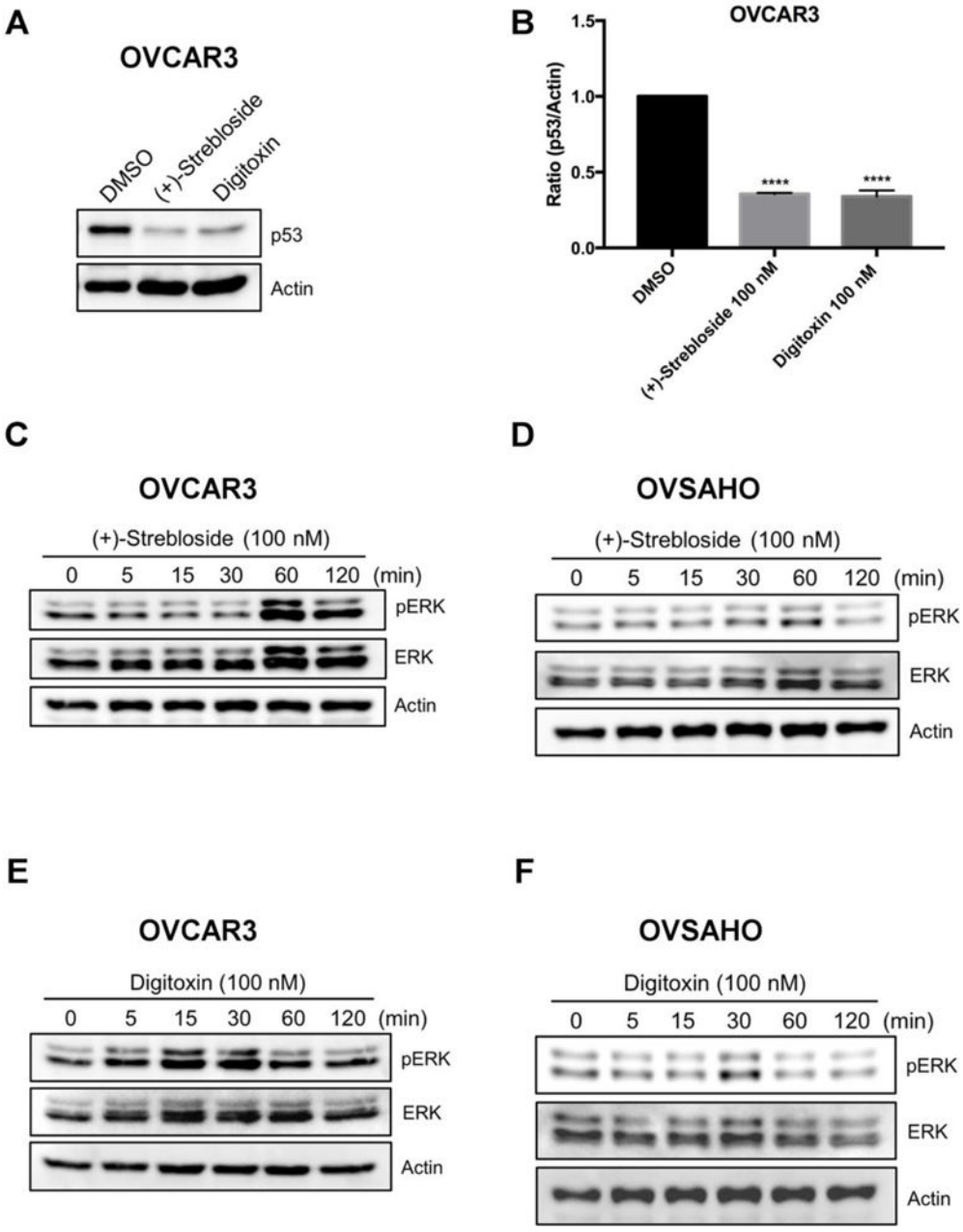

Figure 5.

(+)-Strebloside decreases p53 expression and activates the ERK pathway. (A) OVCAR3 cells were treated with (+)-strebloside or digitoxin at 100 nM for 72 h and subjected to western blot analysis. (B) Quantitative densitometry of western blots indicated significantly decreased expression of p53 in OVCAR3 cells relative to control ($n = 3$). (C and E) OVCAR3 cells were exposed to (+)-strebloside or digoxin at 100 nM for the indicated periods of time, and analyzed by western blotting. (D and F) OVSAHO cells were exposed to (+)-strebloside or digoxin at 100 nM for the indicated periods of time, and analyzed by western blot (**** $p \leq 0.0001$).

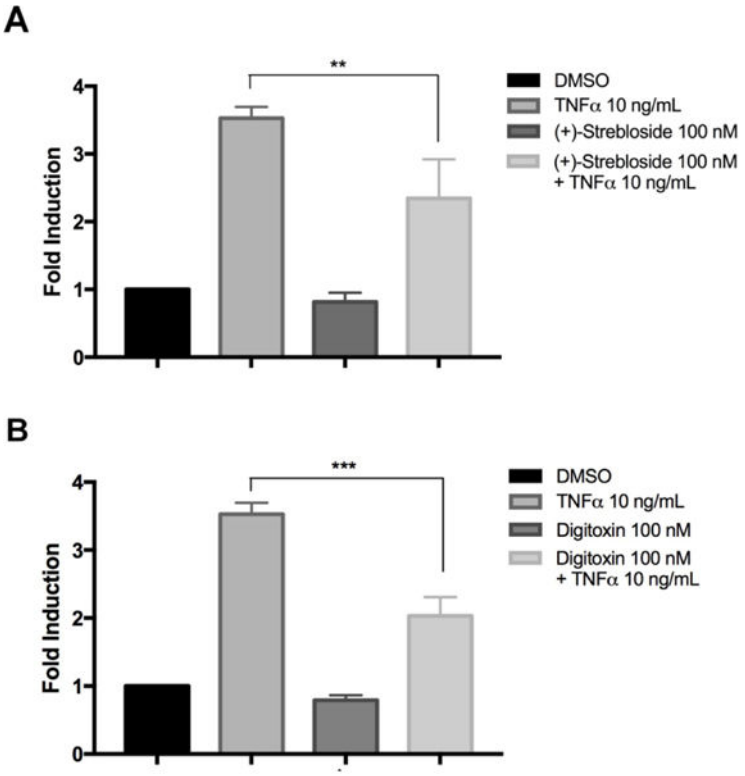

Figure 6.

(+)-Strebloside inhibits NF-κB activation. (A) OVCAR3 cells were transfected with pNF-κB-luc plasmids overnight, then co-treated with 100 nM (+)-strebloside with or without 10 ng/mL TNF-α for 4 h. Cell extracts were collected and analyzed. (B) OVCAR3 cells were transfected with pNF-κB-luc plasmids overnight, then co-treated with 100 nM digitoxin with or without 10 ng/ml TNF-α for 4 h. Cell extracts were collected and analyzed. ANOVA was performed for fold change to analyze significance compared to untreated. Data represented as means ± SEM (** $p \leq 0.01$, *** $p \leq 0.001$).

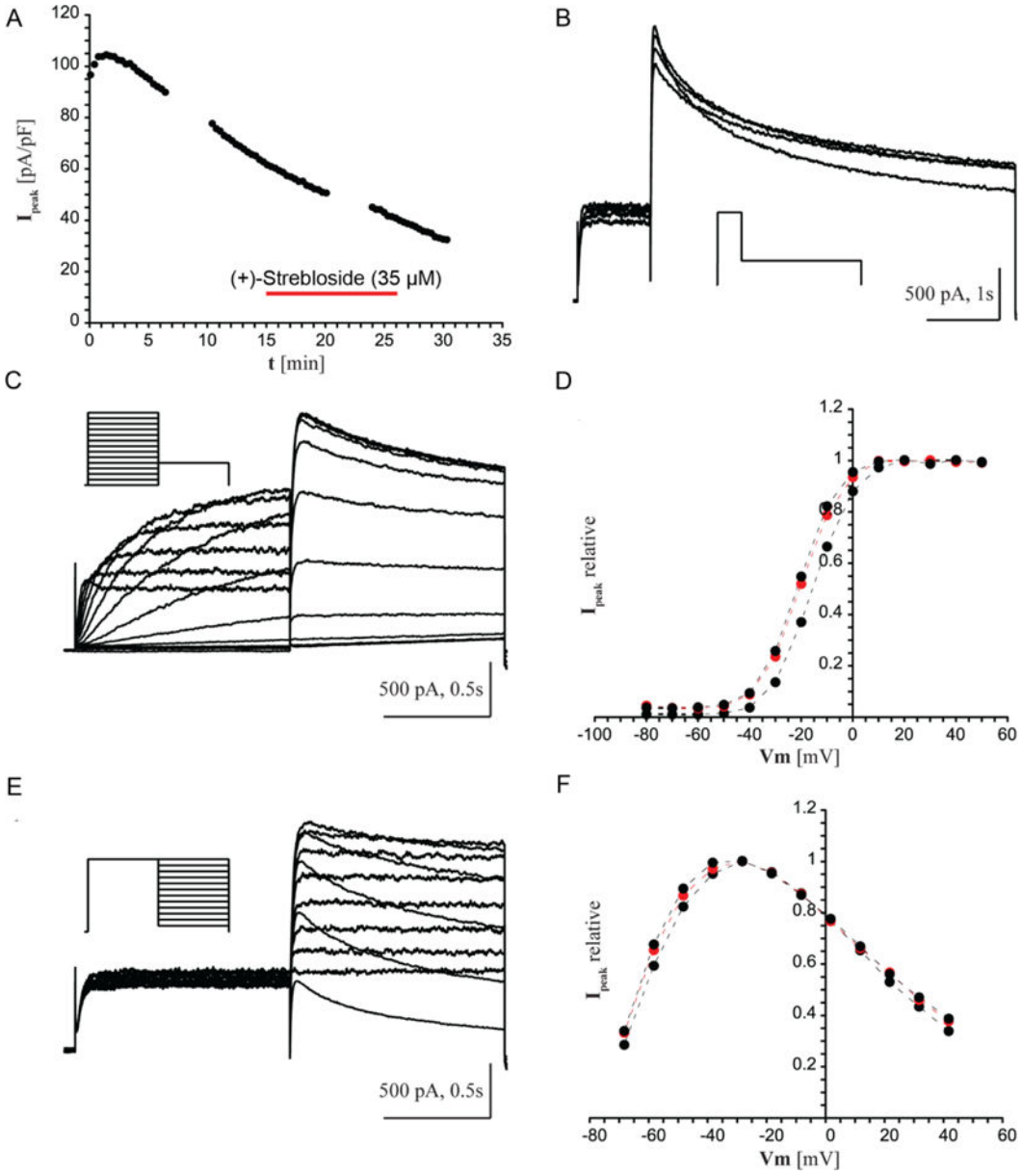

Figure 7.

(+)-Strebloside does not affect hERG1. (A) hERG1 current whole-cell recording over time with example traces and voltage protocol. (B) Example traces and voltage protocol. (C) Current-voltage relationships. **(**D) Activation curve. (E) Voltage-dependence (IV curves were determined during the “gaps” in A). (F) Deactivation curves before, during, and after (+)-strebloside (35 μM) application.

Table 1

Comparative IC_{50} Values of (+)-Strebloside and Digitoxin against Three Human Cancer Cell Lines[a]

cell line	(+)-strebloside (nM)	digitoxin (nM)
MDA-MB-435	78.7	43.3
MDA-MB-231	643.0	482.0
HT-29	101.0	67.6

[a]MDA-MB-435, human melanoma; MDA-MB-231, human breast cancer, HT-29, human colon cancer cells.

Table 2

Comparative IC_{50} Values of (+)-Strebloside and Digitoxin against Six Human High-grade Serous Ovarian Cancer Cell Lines

cell line	(+)-strebloside (nM)	digitoxin (nM)
OVCAR3	134.1	117.1
OVSAHO	560.6	250.2
Kuramochi	3437.0	5911.0
OVCAR4	457.3	425.6
OVCAR5	541.2	321.0
OVCAR8	91.1	71.5

Table 3

Comparative IC_{50} Values of (+)-Strebloside and Digitoxin against Human and Murine Cell Lines

cell line	(+)-strebloside (nM)	digitoxin (nM)
IOSE	50.9	48.4
MOE^{LOW}	$> 5\times10^4$	$> 5\times10^4$
MOE^{HIGH}	$> 5\times10^4$	$> 5\times10^4$
MOE scrambled	$> 5\times10^4$	$> 5\times10^4$
MOE $PTEN^{shRNA}$/$KRAS^{G12V}$	$> 5\times10^4$	$> 5\times10^4$